Available online at www.sciencedirect.com
SCIENCE DIRECT
Tetrahedron
Tetrahedron 61 (2005) 5027–5036

Can a consecutive double turn conformation be considered as a peptide based molecular scaffold for supramolecular helix in the solid state?

Apurba Kumar Das,[a] Arijit Banerjee,[a] Michael G. B. Drew,[b] Sudipta Ray,[a] Debasish Haldar[a] and Arindam Banerjee[a,*]

[a]*Department of Biological Chemistry, Indian Association for the Cultivation of Science, Jadavpur, Kolkata 700 032, India*
[b]*School of Chemistry, The University of Reading, Whiteknights, Reading RG6 6AD, UK*

Received 18 November 2004; revised 21 February 2005; accepted 10 March 2005

Available online 12 April 2005

Abstract—Helices and sheets are ubiquitous in nature. However, there are also some examples of self-assembling molecules forming supramolecular helices and sheets in unnatural systems. Unlike supramolecular sheets there are a very few examples of peptide sub-units that can be used to construct supramolecular helical architectures using the backbone hydrogen bonding functionalities of peptides. In this report we describe the design and synthesis of two single turn/bend forming peptides (Boc-Phe-Aib-Ile-OMe **1** and Boc-Ala-Leu-Aib-OMe **2**) (Aib: α-aminoisobutyric acid) and a series of double-turn forming peptides (Boc-Phe-Aib-Ile-Aib-OMe **3**, Boc-Leu-Aib-Gly-Aib-OMe **4** and Boc-γ-Abu-Aib-Leu-Aib-OMe **5**) (γ-Abu: γ-aminobutyric acid). It has been found that, in crystals, on self-assembly, single turn/bend forming peptides form either a supramolecular sheet (peptide **1**) or a supramolecular helix (peptide **2**), unlike self-associating double turn forming peptides, which have only the option of forming supramolecular helical assemblages.

1. Introduction

The challenge in molecular self-assembly is to design molecular building blocks that are predisposed to give definite supramolecular structures using non-covalent interactions. Supramolecular helices and sheets are the most common and indispensable form of structures in biological systems. Helicity exists in numerous biological and chemical systems. In proteins, the α-helical structure is a very common motif. In DNA-double helices,[1] collagen triple helix[2] and even in the coat protein complex of Tobacco Mosaic Virus (TMV),[3] helicity is a common observable feature. Surprisingly, a considerable amount of helicity is also present in some misfolded, neurodegenerative disease-causing protein aggregates popularly known as amyloid plaques.[4] Unnatural supramolecular helical structures can be constructed using conformational restriction of macromolecules,[5] intra or intermolecular hydrogen bonds[6] or by metal ion chelation.[7] The most common and well-studied example of supramolecular single-, double- and triple-stranded helical conformations are metal chelated, self-assembled, oligonuclear coordination compounds,[7] the helicates.[8] Different approaches to construct supramolecular helices without metal ions and stabilized only by intermolecular and intramolecular hydrogen bonding have also been pursued.[6,9] Recently pyrene-4, 5-dione derivatives have been used to design supramolecular helical structures.[10] Peptide derivatives[11] and even chiral amino acids like the chiral 2,6-pyridinedicarboxamide containing the podand L-histidyl moieties and the corresponding D-derivative[12a] and ferrocene bearing the podand chiral dipeptide moieties (-L-Ala-L-Pro-OEt) and the corresponding D-derivative[12b] have been used to form supramolecular helical assemblages. Parthasarathi and his colleagues have synthesized and characterized a series of tripeptides which form extended helical structures with intervening water molecules between two consecutive peptide molecules and they demonstrated the hydrated helix pattern in crystals.[13] Our group is involved in constructing supramolecular peptide helices utilizing the backbone hydrogen bonding functionalities of the peptide molecules.[14] From our previous report, it has been observed that the short synthetic terminally blocked peptides with single turn/bend conformations can form either supramolecular sheets[15] or supramolecular helices.[14a] However, the peptide molecules with a double turn structure, self-assemble to form

Keywords: Aib; Double turn conformation; 'S' shaped molecular structure; Supramolecular helix.
* Corresponding author. Tel.: +91 33 2473 4971; fax: +91 33 2473 2805; e-mail: bcab@mahendra.iacs.res.in

0040–4020/$ - see front matter © 2005 Elsevier Ltd. All rights reserved.
doi:10.1016/j.tet.2005.03.057

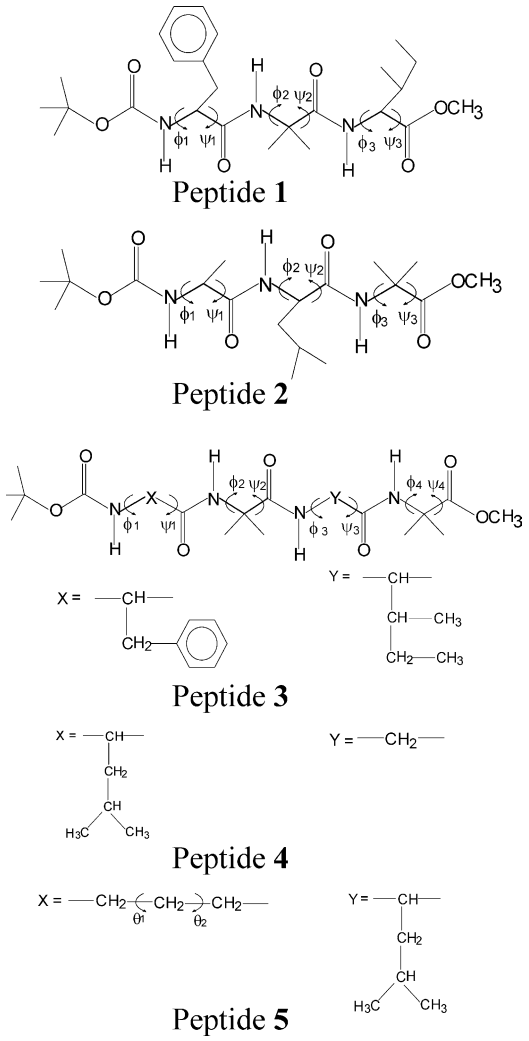

Figure 1. Schematic presentation of peptides **1**–**5**.

supramolecular helices in crystals.[14b–d] Therefore, it is necessary to define the role of a consecutive β-turn structure in the formation of supramolecular helical architecture. In this context we have designed and synthesized a series of single and double turn/ bend forming peptides (Fig. 1). All our previously reported peptides[14,15] and the peptides described in the present work are listed in Table 1. In this paper, we address the question of whether self-assembling double-turn forming peptides can only form supramolecular helical structures or whether other supramolecular architectures are possible.

2. Results and discussion

Peptides (peptides **1**, **2**, **3**, **4** and **5**) reported in this study have been synthesized with conformationally constrained, helicogenic Aib (α-aminoisobutyric acid) residue(s) in order to induce the helical nature of the individual peptide backbone.[16] The terminally protected tripeptides Boc-Phe-Aib-Ile-OMe **1** and Boc-Ala-Leu-Aib-OMe **2** (Fig. 1) have been designed and synthesized to obtain single β-turn/bend forming molecular conformations. The tetrapeptides Boc-Phe-Aib-Ile-Aib-OMe **3** and Boc-Leu-Aib-Gly-Aib-OMe **4** and Boc-γ-Abu-Aib-Leu-Aib-OMe **5**, each containing two Aib residues have been synthesized to obtain double bend conformations with two consecutive β-turns or other unusual turn structures. Previous studies from our group have established that the helix-nucleating Aib (α-aminoisobutyric acid) residue needs to be placed adjacent to the flexible N-terminally located γ-Abu (γ-aminobutyric acid residue) to obtain a turn structure.[17] All the reported peptides were studied using X-ray crystallography, NMR and mass spectrometry.

2.1. Single crystal X-ray diffraction study

Tripeptide **1** contains a helicogenic Aib residue at the central region whereas tripeptide **2** possesses the Aib residue at the C-terminus. The molecular conformations of tripeptides **1** and **2** in the crystal state are illustrated in Figure 2. Most of the ϕ and ψ values (except ψ_1 and ψ_3) of the constituent amino acid residues of tripeptide **1** fall within the helical region of the Ramachandran plot (Table 2). Hence the tripeptide **1** backbone, though it fails to form any intramolecular hydrogen bonded β turn conformation, adopts a bend (turn-like) structure (Fig. 2a), which self-assembles through two intermolecular hydrogen bonds (N6–H6···O8, 2.36 Å, 3.02 Å, 135.00° with symmetry element $-x$, $-0.5+y$, $1-z$) along the crystallographic *b* axis to form a monolayer β-sheet structure. These monolayer structures of tripeptide **1** are further self-assembled into higher order supramolecular β-sheet structure along the crystallographic *a* and *c* directions via van der

Table 1. List of single and double turn/bend forming peptides from our group

Sequence	No. of bends/turns in molecular structure	Supramolecular structure	Reference
1. Boc-Leu-Aib-Phe-OMe	One	Helix	14a
2. Boc-Leu-Aib-Phe-Aib-OMe	Two	Helix	14b
3. Boc-Ala-Aib-Leu-Aib-OMe	Two	Helix	14c
4. Boc-β-Ala-Aib-Leu-Aib-OMe	Two	Helix	14d
5. Boc-Aib-Val-Aib-β-Ala-OMe	Two	Helix	14e
6. Boc-Leu-Aib-β-Ala-OMe	One	Sheet	15a
7. Boc-Ala-Aib-Val-OMe	One	Sheet	15b
8. Boc-Ala-Aib-Ile-OMe	One	Sheet	15b
9. Boc-Ala-Gly-Val-OMe	One	Sheet	15b
10. Boc-Phe-Aib-Ile-OMe	One	Sheet	In current study
11. Boc-Ala-Leu-Aib-OMe	One	Helix	In current study
12. Boc-Phe-Aib-Ile-Aib-OMe	Two	Helix	In current study
13. Boc-Leu-Aib-Gly-Aib-OMe	Two	Helix	In current study
14. Boc-γ-Abu-Aib-Leu-Aib-OMe	Two	Helix	In current study

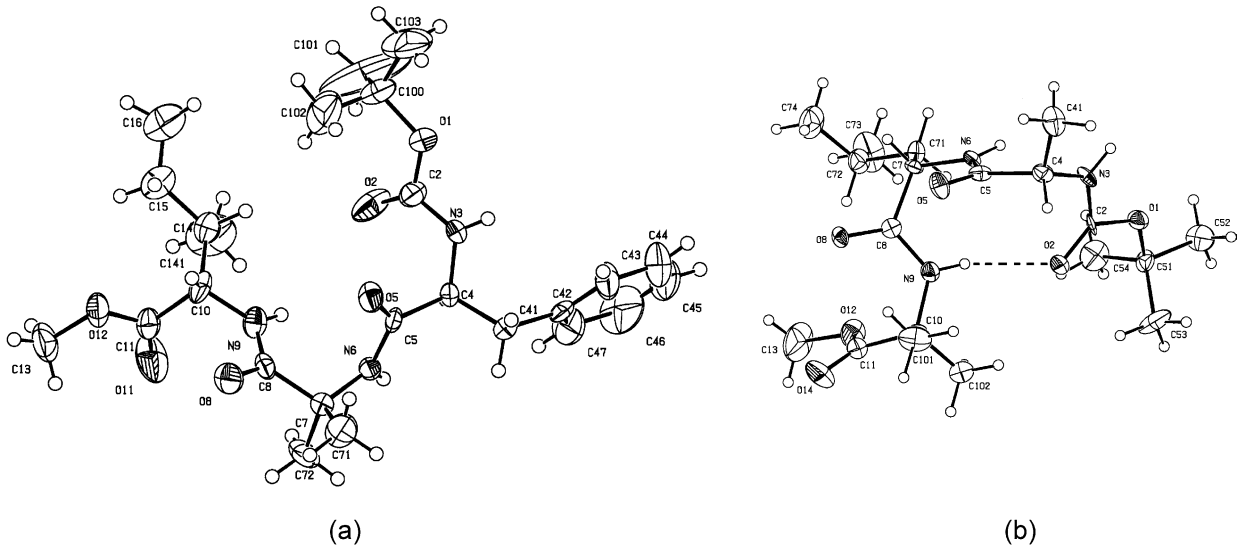

Figure 2. (a) The structure of peptide **1** showing the atomic numbering scheme. Ellipsoids at 30% probability. (b) The ORTEP diagram of the peptide **2** showing the atomic numbering scheme. Ellipsoids at 20% probability. Intramolecular hydrogen bonds are shown as dotted line.

Table 2. Selected backbone torsional angles of peptides **1–5**

Compound	$\phi 1$	$\psi 1$	$\phi 2$	$\psi 2$	$\phi 3$	$\psi 3$	$\phi 4$	$\psi 4$	$\theta 1$	$\theta 2$
Peptide **1**	−59.2	154.2	62.5	30.9	−75.0	146.8	—	—	—	—
Peptide **2**	−66.6	−15.0	−53.5	−42.8	48.2	46.6	—	—	—	—
Peptide **3**	62.0	23.6	53.4	26.6	64.4	25.5	−46.4	134.6	—	—
Peptide **4**	−62.6	116.9	54.8	30.0	83.2	2.6	−47.1	−50.1	—	—
Peptide **5**										
Molecule A	−115.6	−140.8	−53.5	−37.3	−86.5	−6.0	−55.5	−47.8	57.6	64.2
Molecule B	−121.7	−134.8	−55.5	−37.3	−80.2	−14.0	42.5	−128.4	60.2	56.6

Waals interactions (Fig. 3). By comparison Figure 2b shows that there is a 4→1 hydrogen bond between Boc CO and Aib(3) N–H (N9–H···O2, 2.37, 3.04 Å, 135.00°) forming a distorted type III β-turn (10-membered hydrogen bonded ring) conformation in tripeptide **2**. The backbone torsion angles of tripeptide **2** fall within the helical region of the Ramachandran plot (Table 2). For the first two residues, that is Ala(1) and Leu(2), the ϕ, ψ values lie within the right handed helical region of the Ramachandran plot while ϕ, ψ values of the last residue (Aib(3)) fall in the left-handed helical region. Each individual sub-unit of tripeptide **2** then self-assembles through intermolecular hydrogen bonds (N3–H···O8, 2.11, 2.93 Å, 159.00° and N6–H···O5, 2.37, 3.2 Å, 164.00° with symmetry element $-0.5+x$, $-0.5-y$, $-z$) atop one another to form a supramolecular helix along the crystallographic *a* axis (Fig. 4). In the former example and other previous studies[15] it has been demonstrated that tripeptides with single β-turn conformations can form supramolecular β-sheet architectures upon self-assembly. The structure of peptide **2** reported here and other earlier work in the literature[14a] has indicated that tripeptides containing a turn/bend conformation can also form supramolecular helical structure upon self-association in the solid state. So, molecular self-assembly of single-turn forming peptides does not only lead to one particular type of supramolecular structure, but can form either supramolecular helices or supramolecular β-sheets depending upon the nature of crystal packing.

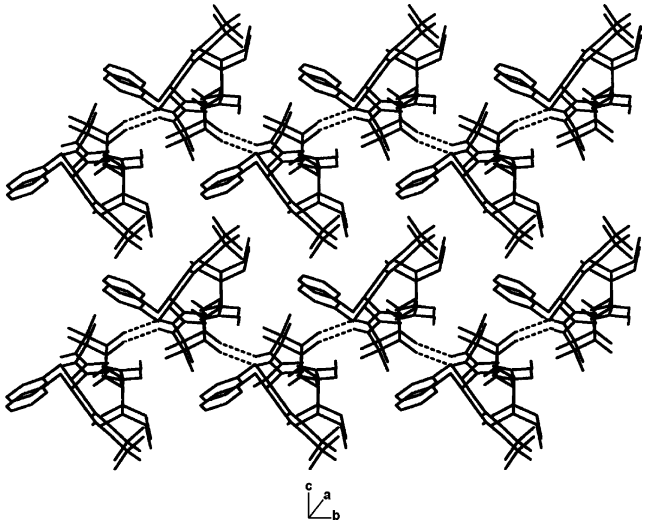

Figure 3. Packing of peptide **1** along crystallographic *b* axis showing intermolecularly hydrogen bonded sheet-like structure.

We are trying to find a peptide-based molecular scaffold, which can only form a definite type of supramolecular structure: namely the supramolecular helix. In this regard we have designed and synthesized tetrapeptides **3**, **4** and **5**. From X-ray crystallography, it is evident that the tetrapeptide **3** adopts a consecutive β-turn structure in the crystal (Fig. 5a). Incorporation of helicogenic Aib residues has driven the tetrapeptide **3** backbone to form two overlapping type III′ β-turn conformations through intramolecular

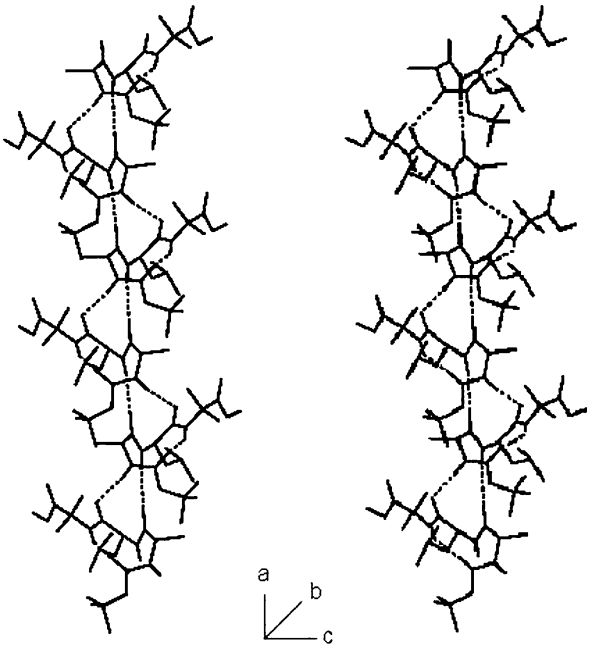

Figure 4. A cross-eye stereo representation of the higher order packing of peptide **2** along crystallographic *a* axis showing the formation of supramolecular helix via intermolecular hydrogen bonds.

hydrogen bonds (N9–H···O2, 2.31, 3.17 Å, 175.00° and N12–H···O5, 2.17 Å, 2.95 Å, 151.00°). Most of the backbone torsion angles (except $\psi 4$) of tetrapeptide **3** are in the left-handed helical region of the Ramachandran diagram (Table 2). The tetrapeptide **4** also forms two successive β-turns in the crystal (Fig. 5b). Ten-membered intramolecular hydrogen bonds are formed between the CO of the Boc group and Gly(3) NH (N13–H···O4, 2.21, 3.02 Å, 157.00°) and the CO of Leu(1) and Aib(4) NH (N17–H···O7, 2.05 Å, 2.88 Å, 162.00°), respectively, in tetrapeptide **4**. The backbone torsion angles (except ψ_1) of tetrapeptide **4** are mostly in the helical region of the Ramachandran diagram

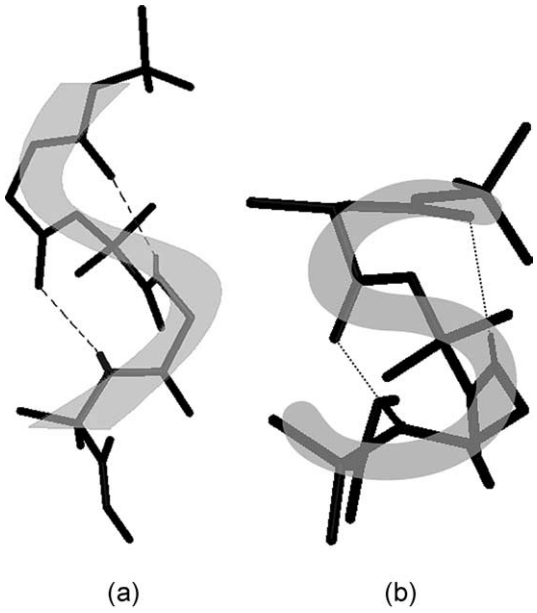

Figure 5. (a) Formation of 'S' shaped molecular scaffold by peptide **3** and (b) Formation of 'S' shaped molecular scaffold by peptide **4**.

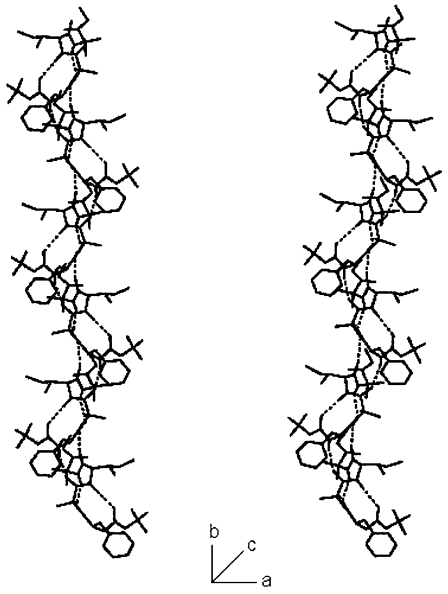

Figure 6. Cross-eye stereo representation of the packing of peptide **3** shows the intermolecular hydrogen-bonded supramolecular helix along the *b* axis. Hydrogen bonds are shown as dotted lines.

(Table 2). However, the dihedral angles of tetrapeptide **4** indicate that the first turn is a type II β-turn whereas the second turn is a type I′ β-turn. In both tetrapeptides **3** and **4**, the Aib(2) residue occupies simultaneously the $i+2$th position of first turn and the $i+1$th position of the second turn. Here the remarkable feature is that these two tetrapeptides form an 'S' shaped molecular scaffold as a result of the double turn structure (Fig. 5). The individual tetrapeptide **3** subunits are regularly stacked atop one another through multiple intermolecular hydrogen bonds (N6–H···O11, 2.23, 2.95 Å, 141.00° and N4–H···O8, 2.10 Å, 2.90 Å, 154.00° with symmetry element $1-x$, $0.5+y$, $0.5-z$) to form a supramolecular helix along the axis parallel to crystallographic *b* direction (Fig. 6). The hydrogen bonds between the Phe(1) and Aib(2) NH groups and the Aib(2) and Ile(3) C═O groups are responsible for connecting individual molecules to form and stabilize the supramolecular one-dimensional helical column of peptide **3**. The supramolecular building blocks of tetrapeptide **4** are further self-assembled through selective intermolecular hydrogen bonds (N5–H···O16, 2.01, 2.86 Å, 174.00° with symmetry element $2-x$, $0.5+y$, $0.5-z$) to generate a supramolecular helical architecture along the crystallographic *b* axis (Fig. 7). One interesting feature of the crystal structure of the tetrapeptide **4** is that, the individual helical columns of **4** are linked to the adjacent column exploiting the hydrogen bond functionalities of Aib(2) NH and Aib(4) CO (N8–H···O20, 2.09, 2.93 Å, 165.00° with symmetry element $1+x$, y, z).

The molecular conformation of tetrapeptide **5** (Fig. 8) was also established by single crystal X-ray diffraction studies. Figure 8 illustrates that there are two molecules (namely A and B) in the asymmetric unit, which have equivalent conformations. Both molecules A and B in the asymmetric unit form a hydrogen bond to a water molecule (N3A–H···O200, 2.18, 3.00 Å, 160.00° for molecule A and N3B–H···O100, 2.22, 3.04 Å, 160.00° for molecule B with symmetry

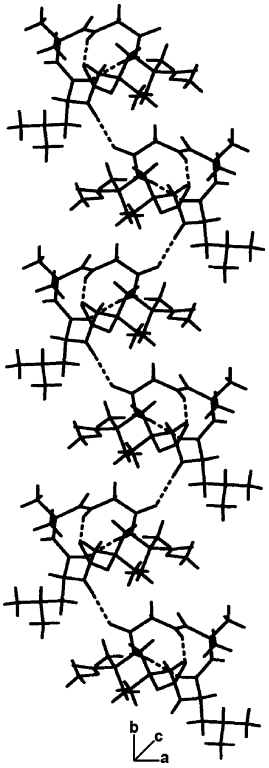

Figure 7. The packing of the peptide **4** illustrating the intermolecular hydrogen-bonded supramolecular helix along the *b* axis. Hydrogen bonds are shown as dotted lines.

equivalent x, $-1+y$, z and x, $1+y$, z, respectively). The insertion of two CH_2 groups into the backbone (γ-Abu) causes an unusual $4\rightarrow1$ type hydrogen bond (N11A–H···O2A, 2.24, 3.07 Å, 163.00° for molecule A and N11B–H···O2B, 2.19, 3.03 Å, 165.00° for molecule B) between the CO of the Boc group and the NH of Leu(3) forming a 12-membered hydrogen bonded ring (Fig. 8). An additional 10-atom hydrogen bonded β-turn (N18A–H···O7A, 2.18, 3.02 Å, 165.00° for molecule A and N18B–H···O7B, 2.26, 3.05 Å, 152.00° for molecule B) between the CO of γ-Abu and the NH of Aib(4) is also formed adjacent to the 12-membered hydrogen bonded ring. Hence, tetrapeptide **5** also has a double bend 'S' shaped molecular conformation. Most of the ϕ and ψ values (except ϕ_1 and ψ_1 of molecule A and ϕ_1, ψ_1 and ψ_4 of molecule B) of the constituent amino acid residues of tetrapeptide **5** fall within the helical region of Ramachandran plot (Table 2). The torsions about the polymethylene groups of the N-terminal γ-Abu residue (namely θ_1 and θ_2) in peptide **5** are in *gauche* conformation. The peptide self-assembles through intermolecular hydrogen bonds (N8A–H···O10A, 2.15, 2.92 Å, 149.00° with symmetry equivalent $0.5-x$, $-0.5+y$, $1-z$ for molecule A and N8B–H···O10B, 2.15, 2.92 Å, 149.00° with symmetry equivalent $0.5-x$, $0.5+y$, $-z$ for molecule B) maintaining the proper registry of molecules A and B along the crystallographic *b* axis to form a supramolecular helical structure (Fig. 9). Crystal data for all the reported peptides are listed in Table 3.

3. Conclusion

All the reported peptides are composed of one or more conformationally constrained Aib residues and their backbone dihedral angles demonstrate that they mostly adopt helical conformations. Crystallographic studies of tripeptides **1** and **2** demonstrate that the self-association of peptides containing only one turn have two options to form a supramolecular architecture: either a supramolecular sheet or a supramolecular helix. Tetrapeptides **3** and **4** share a common structural motif, consecutive double bend molecular conformations and self-association of each peptide

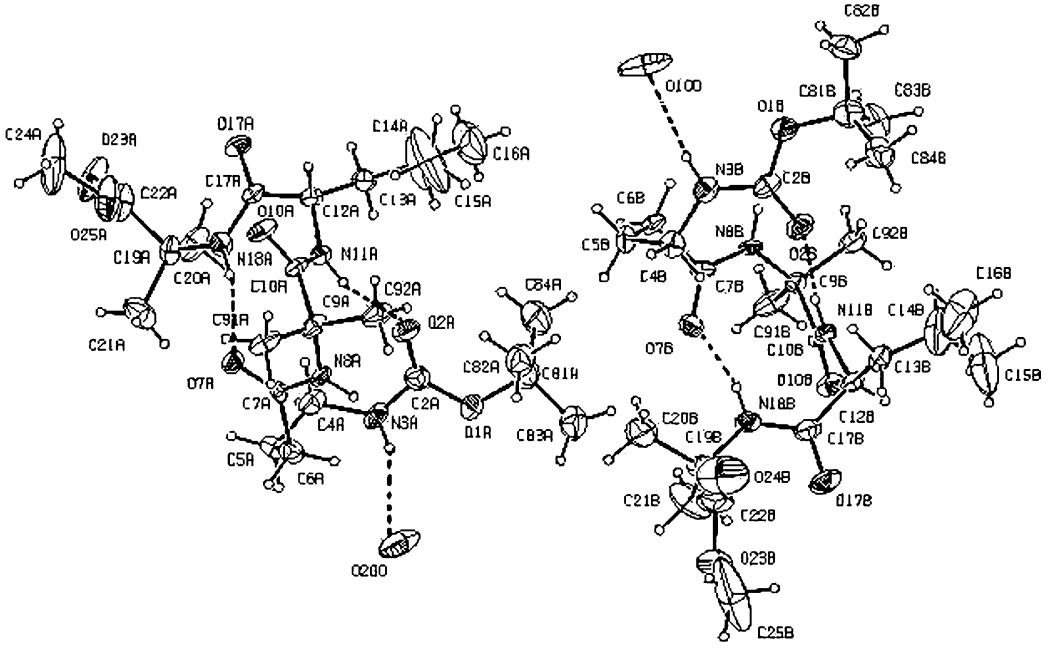

Figure 8. Molecular conformation of peptide **5** with atom numbering scheme. The asymmetric unit contains two molecules (namely A and B) each of which has a water molecule. Each molecule forms a 12 membered unusual turn adjacent with a 10 membered distorted type III β-turn. The hydrogen bonds are shown as dotted line. Thermal ellipsoids are shown at the level of 20% probability.

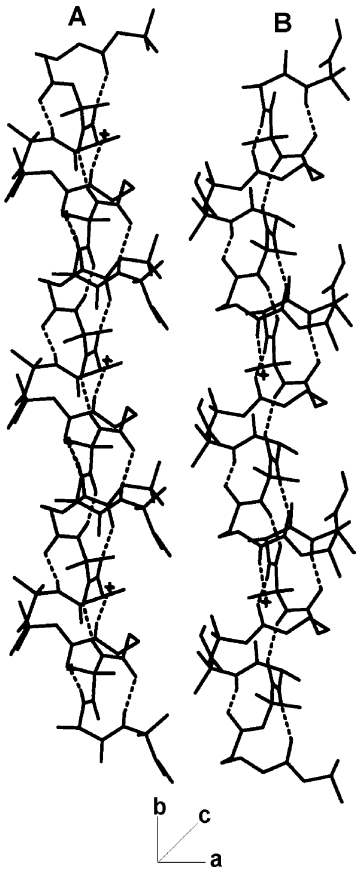

Figure 9. Packing diagram of peptide **5** along the crystallographic *b* axis showing intermolecular hydrogen-bonded supramolecular helices. The A and B molecules packed through proper registry, individual helix is formed by only a particular molecule that is either molecule A or B. Intermolecular hydrogen bonds are shown as dotted lines. The hydrogen bonded water molecule with each peptide is shown as *.

create supramolecular helices in crystals. Tetrapeptide **5**, instead of having a conformationally flexible γ-amino-butyric acid residue at the N terminus, also forms a double bend molecular conformation with two consecutive turns; one of which is an unusual turn with a 12-atom hydrogen bonded ring structure followed by a classical β-turn conformation. Thus, all these tetrapeptides, despite substantial differences in sequences adopt a double turn conformation, which in turn leads to the formation of a common S shaped molecular structure. This S shaped structure may increase the inherent propensity of individual tetrapeptide subunits to form a supramolecular helical architecture through intermolecular hydrogen bonds in the solid state.

Our work offers an elegant approach to controlling the three-dimensional structure using the stereochemical nature of a conformationally constrained amino acid (viz. Aib). This study should be useful for designing and calibrating supramolecular architectures having importance both in supramolecular chemistry and crystal engineering.

4. Experimental

4.1. Synthesis of peptide 1

4.1.1. Boc-Phe(1)-OH 6. A solution of phenylalanine (4.95 g, 30 mmol) in a mixture of dioxane (60 mL), water (30 mL) and 1 M NaOH (30 mL) was stirred and cooled in an ice-water bath. Di-*tert*-butyldicarbonate (7.2 g, 33 mmol) was added and stirring was continued at room temperature for 6 h. Then the solution was concentrated under vacuum to about 40–60 mL, cooled in an ice water bath, covered with a layer of ethyl-acetate (about 50 mL) and acidified with a dilute solution of $KHSO_4$ to pH 2–3 (Congo red). The aqueous phase was extracted with ethyl acetate and this operation was done repeatedly. The ethyl acetate extracts were pooled, washed with water and dried over anhydrous Na_2SO_4 and evaporated under vacuum. The pure material as white solid was obtained.

Yield=96% (7.63 g, 28.8 mmol). Mp 85–87 °C. Elemental Analysis Calcd for $C_{14}H_{19}NO_4$ (265): C, 63.50; N, 5.24; H, 7.20. Found: C, 63.39; N, 5.28; H, 7.17.

4.1.2. Boc-Phe(1)-Aib(2)-OMe 7. Boc-Phe-OH (7.42 g 28 mmol) was dissolved in a mixture of 30 mL dichloromethane (DCM) in an ice-water bath. H-Aib-OMe was isolated from the corresponding methyl ester hydrochloride (8.6 g, 56 mmol) by neutralization and subsequent extraction with ethyl acetate and the ethyl acetate extract was

Table 3. Crystal and data collection parameters of peptides **1**–**5**

	Peptide **1**	Peptide **2**	Peptide **3**	Peptide **4**	Peptide **5**
Empirical formula	$C_{25}H_{39}N_3O_6$	$C_{19}H_{35}N_3O_6$	$C_{29}H_{46}N_4O_7$	$C_{22}H_{40}N_4O_7$	$C_{24}H_{44}N_4O_7$, H_2O
Crystallizing solvent	Methanol–water	Methanol–water	Methanol–water	Methanol–water	Methanol–water
Crystal system	Monoclinic	Orthorhombic	Orthorhombic	Orthorhombic	Monoclinic
Space group	$P2_1$	$P2_12_12_1$	$P2_12_12_1$	$P2_12_12_1$	$C2$
a (Å)	10.224(11)	10.613(12)	10.179(12)	10.421(17)	29.557(3)
b (Å)	11.378(12)	10.476(12)	15.606(17)	13.361(2)	12.237(14)
c (Å)	12.578(14)	21.132(2)	20.727(23)	20.171(3)	20.703(2)
β (°)	105.28(10)	(90)	(90)	(90)	121.31(1)
U (Å^3)	1411.5	2349.50	3292.55	2808(7)	6397.21
Z	2	4	4	4	8
Mol. Wt.	477.59	401.50	562.7	472.58	516.63
Density (Calcd, mg/mm^3)	1.124	1.135	1.135	1.117	1.073
Unique data	5066	3249	5268	4296	9986
Observed reflns. ($I>2\sigma(I)$)	3291	1757	1994	2701	4607
R	0.0881	0.1157	0.1015	0.0839	0.1178
*wR*2	0.1331	0.2915	0.2014	0.2394	0.2280
Largest diff. peak and hole (e/Å^3)	0.259, −0.180	0.376, −0.321	0.269–0.260	0.204, −0.205	0.370, −0.251

concentrated to 10 mL. This was added to the reaction mixture, followed immediately by di-cyclohexylcarbodiimide (DCC) (5.77 g, 28 mmol). The reaction mixture was allowed to come to room temperature and stirred for 24 h. DCM was evaporated, and the residue was taken up in ethyl acetate (60 mL), and dicyclohexylurea (DCU) was filtered off. The organic layer was washed with 2 M HCl (3×50 mL), brine, then 1 M sodium carbonate (3×50 mL) and brine (2×50 mL) and dried over anhydrous sodium sulfate, and evaporated under vacuum to yield 8.74 g (24 mmol, 86%) of **7** as white solid.

Yield=86% (8.74 g, 24 mmol). Mp 119–121 °C. ^{1}H NMR ($CDCl_3$, 300 MHz, δ ppm): 7.22–7.35 (m, 5H); 6.3 (s, 1H); 5.1 (d, J=9 Hz, 1H); 4.28 (m, 1H); 3.71 (s, 3H); 2.96–3.07 (m, 2H); 1.45 (s, 6H); 1.42 (s, 9H). Elemental Analysis Calcd for $C_{19}H_{28}N_2O_5$ (364): C, 62.45; N, 7.72; H, 7.71. Found: C, 62.63; N, 7.69; H, 7.69.

4.1.3. Boc-Phe(1)-Aib(2)-OH 8. To **7** (8.5 g 23.35 mmol), MeOH (50 mL) and 2 M NaOH (20 mL) were added and the progress of saponification was monitored by thin layer chromatography (TLC). The reaction mixture was stirred at room temperature. After 10 h methanol was removed under vacuum, the residue was taken up in 50 mL of water, washed with diethyl ether (2×50 mL). Then the pH of the aqueous layer was adjusted to 2 using 1 M HCl and it was extracted with ethyl acetate (3×50 mL). The extracts were pooled, dried over anhydrous sodium sulfate, and evaporated in vacuum to yield a waxy solid.

Yield=92% (7.525 g, 21.5 mmol). ^{1}H NMR ($(CD_3)_2SO$, 300 MHz, δ ppm): 12.27 (br, 1H); 8.05 (s, 1H); 7.17–7.26 (m, 5H); 6.77 (d, J=9 Hz, 1H); 4.13–4.21 (m, 1H); 2.85–3.02 (m, 2H); 1.34 (s, 6H); 1.29 (s, 9H). Elemental Analysis Calcd for $C_{18}H_{26}N_2O_5$ (350): C, 61.60; N, 7.96; H, 7.56. Found: C, 61.71; N, 8.00; H, 7.43.

4.1.4. Boc-Phe(1)-Aib(2)-Ile(3)-OMe 1. Boc-Phe(1)-Aib(2)-OH (7 g, 20 mmol) in DMF (15 mL) was cooled in an ice-water bath and H-Ile-OMe was isolated the corresponding methyl ester hydrochloride from (7.26 g, 40 mmol) by neutralization and subsequent extraction with ethyl acetate and the ethyl acetate extract was concentrated to 8 mL. It was then added to the reaction mixture, followed immediately by 4.12 g (20 mmol) DCC and HOBt (2.7 g, 20 mmol). The reaction mixture was stirred for 3 days. The residue was taken up in ethyl acetate (40 mL) and the DCU was filtered off. The organic layer was washed with 2 M HCl (3×40 mL), brine, 1 M sodium carbonate (3×40 mL), brine (2×40 mL), dried over anhydrous sodium sulfate and evaporated in vacuum to yield 8.1 g (17 mmol) of white solid. Purification was done by silica gel column (100–200 mesh) using ethyl acetate as eluent. Colorless single crystals were grown from methanol/water solvent system (methanol/water=80:20) by slow evaporation.

Yield=85%, (8.1 g, 17 mmol). R_f (ethyl acetate) 0.78. Mp 104–106 °C. ν_{max} (KBr)/cm^{-1} 1655, 1697, 3321, 3395, 3427. ^{1}H NMR ($CDCl_3$, 300 MHz, δ ppm): 7.22–7.35 (m, 5H); 7.01 (d, J=9 Hz, 1H); 6.17 (s, 1H); 5.07 (d, J=9 Hz, 1H); 4.54–4.50 (m, 1H); 4.28–4.20 (m, 1H); 3.72 (s, 3H); 3.08–3.03 (m, 2H); 1.93–1.88 (m, 1H); 1.42 (s, 9H); 1.39 (s, 6H); 1.25–1.13 (m, 2H); 0.89–0.94 (m, 6H). ^{13}C NMR ($CDCl_3$, 300 MHz, δ ppm): 173.58, 172.17, 170.65, 136.56, 129.15, 129.06, 128.58, 126.87, 80.24, 57.16, 56.56, 51.83, 37.49, 28.05, 25.40, 24.90, 24.80, 24.38, 15.33, 11.37. $[\alpha]_D^{25.7}=+5.57$ (c 2.07, $CHCl_3$). Mass Spectral data $(M+Na)^+=500.7$, $M_{Calcd}=477$. Elemental Analysis Calcd for $C_{25}H_{39}N_3O_6$ (477): C, 66.89; N, 8.80; H, 8.47. Found: C, 66.81; N, 8.85; H, 8.53.

4.1.5. Boc-Ala(1)-OH 9. See Ref. 15b.

4.1.6. Boc-Ala(1)-Leu(2)-OMe 10. Boc-Ala-OH (5.67 g, 30 mmol) was dissolved in a mixture of dichloromethane (DCM) (30 mL) in an ice-water bath. H-Leu-OMe was isolated from the corresponding methyl ester hydrochloride (10.89 g, 60 mmol) by neutralization and subsequent extraction with ethyl acetate and the ethyl acetate extract was concentrated to 10 mL. This was added to the reaction mixture, followed immediately by di-cyclohexylcarbodiimide (DCC) (6.18 g, 30 mmol). The reaction mixture was allowed to come to room temperature and stirred for 24 h. DCM was evaporated, and the residue was taken up in ethyl acetate (60 mL), and dicyclohexylurea (DCU) was filtered off. The organic layer was washed with 2 M HCl (3×50 mL), brine, then 1 M sodium carbonate (3×50 mL) and brine (2×50 mL) and dried over anhydrous sodium sulfate, and evaporated under vacuum to yield **10** as waxy solid.

Yield=83.3% (7.9 g, 25 mmol). ^{1}H NMR ($CDCl_3$, 300 MHz, δ ppm): 6.71 (d, J=6 Hz, 1H); 5.15 (d, J=7.5 Hz, 1H); 4.64–4.57 (m, 1H); 4.15–4.11 (m, 1H); 3.74 (s, 3H); 1.61–1.69 (m, 3H); 1.45 (s, 9H); 1.35 (m, 3H); 0.93 (m, 6H). Elemental Analysis Calcd for $C_{15}H_{28}N_2O_5$ (316): C, 56.85; N, 8.72; H, 8.90. Found: C, 56.96; N, 8.86; H, 8.86.

4.1.7. Boc-Ala(1)-Leu(2)-OH 11. To **10** (6.32 g, 20 mmol), MeOH (50 mL) and 2 M NaOH (20 mL) were added and the progress of saponification was monitored by thin layer chromatography (TLC). The reaction mixture was stirred at room temperature. After 10 h methanol was removed under vacuum, the residue was taken up in 50 mL of water, washed with diethyl ether (2×50 mL). Then the pH of the aqueous layer was adjusted to 2 using 1 M HCl and it was extracted with ethyl acetate (3×50 mL). The extracts were pooled, dried over anhydrous sodium sulfate, and evaporated under vacuum to yield 4.23 g of **11** as white solid.

Yield=70% (4.23 g, 14 mmol). Mp 124–126 °C. ^{1}H NMR ($(CD_3)_2SO$, 300 MHz, δ ppm): 12.41 (br, 1H); 7.88 (d, J=9 Hz, 1H); 6.85 (d, J=6 Hz, 1H); 4.24–4.17 (m, 1H); 3.99–3.94 (m, 1H); 1.49–1.66 (m, 3H); 1.35 (s, 9H); 1.14 (m, 3H); 0.81–0.88 (m, 6H). Elemental Analysis Calcd for $C_{14}H_{26}N_2O_5$ (302): C, 55.60; N, 9.21; H, 8.56. Found: C, 55.63; N, 9.27; H, 8.60.

4.1.8. Boc-Ala(1)-Leu(2)-Aib(3)-OMe 2. Boc-Ala(1)-Leu(2)-OH (2.74 g, 10 mmol) in DMF (15 mL) was cooled in an ice-water bath and H-Aib-OMe was isolated from the corresponding methyl ester hydrochloride (3.07 g, 20 mmol) by neutralization and subsequent extraction with ethyl acetate and the ethyl acetate extract was concentrated to 8 mL. It was then added to the reaction mixture, followed immediately by DCC (2.06 g, 10 mmol) and HOBt (1.35 g,

10 mmol). The reaction mixture was stirred for 3 days. The residue was taken up in ethyl acetate (40 mL) and the DCU was filtered off. The organic layer was washed with 2 M HCl (3×40 mL), brine, 1 M sodium carbonate (3×40 mL), brine (2×40 mL), dried over anhydrous sodium sulfate and evaporated under vacuum to yield 3.21 g (8 mmol) of white solid. Purification was done by silica gel column (100–200 mesh) using ethyl acetate–toluene (3:1) as eluent. Colorless single crystals were grown from methanol/water solvent system (methanol/water=90:10) by slow evaporation.

Yield=80% (3.21 g, 8 mmol). R_f (25% toluene/ethyl acetate) 0.68. Mp 117–119 °C. ν_{max} (KBr)/cm^{-1} 1659, 1684, 1753, 3244, 3321, 3350. ^{1}H NMR ($CDCl_3$, 300 MHz, δ ppm): 6.84 (s, 1H); 6.60 (d, J=9 Hz, 1H); 5.00 (d, J=6 Hz, 1H); 4.44–4.36 (m, 1H); 4.16–4.12 (m, 1H); 3.71 (s, 3H); 1.59–1.73 (m, 3H); 1.50 (s, 3H); 1.53 (s, 3H); 1.45 (s, 9H); 1.37 (d, J=9 Hz, 3H); 0.90–0.94 (m, 6H). ^{13}C NMR ($CDCl_3$, 300 MHz, δ ppm): 174.52, 172.73, 170.85, 155.44, 80.08, 56.07, 52.28, 51.44, 40.27, 28.09, 24.60, 24.56, 24.48, 24.39, 22.76, 21.76, 15.00. $[\alpha]_D^{25.7}=-57.27$ (c 2.10, $CHCl_3$). Mass Spectral data $(M+Na+H)^+=425.1$, $M_{Calcd}=401$. Elemental Analysis Calcd for $C_{19}H_{35}N_3O_6$ (401): C, 56.85; N, 10.47; H, 8.72. Found: C, 56.81; N, 10.85; H, 8.53.

4.1.9. Boc-Phe(1)-Aib(2)-Ile(3)-OH 12. To Boc-Phe(1)-Aib(2)-Ile(3)-OMe **1** (5 g, 10.48 mmol), methanol (50 mL) and of 2 M NaOH (20 mL) were added and the progress of saponification was monitored by thin layer chromatography (TLC). The reaction mixture was stirred at room temperature. After 10 h methanol was removed under vacuum, the residue was taken in 50 mL of water, washed with diethyl ether (2×50 mL). Then pH of the aqueous layer was adjusted to 2 by adding 1 M HCl and it was extracted with ethyl acetate (3×40 mL). The extracts were pooled, dried over anhydrous sodium sulfate and evaporated under vacuum to yield a waxy solid.

Yield=89% (4.32 g, 9.33 mmol). ^{1}H NMR ($(CD_3)_2SO$, 300 MHz, δ ppm): 12.52 (br, 1H); 7.95 (s, 1H); 7.28–7.35 (m, 5H); 7.21 (d, J=9 Hz, H); 6.9 (d, J=9 Hz, 1H); 4.36–4.44 (m, 1H); 4.16–4.12 (m, 1H); 2.87–2.96 (m, 2H); 1.77–1.89 (m, 1H); 1.30 (s, 6H); 1.28 (s, 9H); 1.07–1.18 (m, 2H); 0.81–0.82 (m, 6H). Elemental Analysis Calcd for $C_{24}H_{37}N_3O_6$ (463): C, 62.26; N, 9.02; H, 8.02. Found: C, 62.20; N, 9.07; H, 7.99.

4.1.10. Boc-Phe(1)-Aib(2)-Ile(3)-Aib(4)-OMe 3. To **12** (4.2 g, 9.1 mmol) in DMF (10 mL) was cooled in an ice water bath. H-Aib-OMe was isolated from the corresponding methyl ester hydrochloride (2.8 g, 18.2 mmol) by neutralization, subsequent extraction with ethyl acetate and concentration (7 mL) and this was added to the reaction mixture, followed immediately by DCC (1.87 g, 9.1 mmol) and HOBt (1.23 g, 9.1 mmol). The reaction mixture was stirred for 3 days. The residue was taken in ethyl acetate (50 mL) and DCU was filtered off. The organic layer was washed with 2 M HCl (3×50 mL), brine, 1 M sodium carbonate (3×50 mL), brine (2×50 mL), dried over anhydrous sodium sulfate and evaporated under vacuum to yield 4.14 g (7.37 mmol, 81%) of white solid. Purification was done by silica gel column (100–200 mesh) using ethyl acetate–toluene (3:1) as eluent. Colorless single crystals were obtained from methanol–water (90:10) by slow evaporation.

Yield=81% (4.14 g, 7.37 mmol). R_f (25% toluene/ethyl acetate) 0.65. Mp 168–170 °C. ν_{max} (KBr)/cm^{-1} 1647, 1730, 1747, 3308, 3551. ^{1}H NMR ($CDCl_3$, 300 MHz δ ppm): 7.20–7.34 (m, 5H); 7.13 (s, 1H); 6.64 (d, J=9 Hz, 1H); 6.31 (s, 1H); 5.01 (d, J=7 Hz, 1H); 4.44 (m, 1H); 4.11–4.14 (m, 1H); 3.70 (s, 3H); 3.07–3.11 (m, 2H); 2.22 (m, 1H); 1.56, 1.53 (s, 6H); 1.43 (s, 9H); 1.26 (s, 6H); 0.89–0.91 (m, 6H). ^{13}C NMR ($CDCl_3$, 300 MHz, δ ppm): 174.89, 173.64, 171.19, 170.37, 155.82, 129.13, 129.02, 128.87, 128.78, 128.61, 127.19, 80.91, 57.93, 56.91, 55.80, 52.03, 27.92, 25.20, 25.03, 24.42, 24.35, 23.99, 15.53, 15.47, 11.57, 11.51, 11.49. $[\alpha]_D^{25.7}=-15.35$ (c 2.10, $CHCl_3$). Mass Spectral data $(M+Na+2H)^+=587.8$, $M_{Calcd}=562.7$. Elemental Analysis Calcd for $C_{29}H_{46}N_4O_7$ (562): C, 62.02; N, 9.91; H, 8.12. Found: C, 61.90; N, 9.96; H, 8.19.

4.1.11. Boc-Leu(1)-OH 13. See Ref. 18.

4.1.12. Boc-Leu(1)-Aib(2)-OMe 14. See Ref. 18.

4.1.13. Boc-Leu(1)-Aib(2)-OH 15. See Ref. 18.

4.1.14. Boc-Leu(1)-Aib(2)-Gly(3)-OBz 16. Boc-Leu(1)-Aib(2)-OH (6.32 g, 20 mmol) in DMF (20 mL) was cooled in an ice-water bath and H-Gly-OBz was isolated from the corresponding benzyl ester p-toluenesulfonate (8.62 g, 40 mmol) by neutralization, subsequent extraction with ethyl acetate and concentration (10 mL) and it was added to the reaction mixture, followed immediately by DCC (4.12 g, 20 mmol) and HOBt (2.7 g, 20 mmol). The reaction mixture was stirred for 3 days. The residue was taken in ethyl acetate (60 mL) and the DCU was filtered off. The organic layer was washed with 2 M HCl (3×50 mL), brine, 1 M sodium carbonate (3×50 mL), brine (2×50 mL), dried over anhydrous sodium sulfate and evaporated under vacuum to yield 8.11 g (17 mmol) of **16** as waxy solid.

Yield=81% (7.87 g, 17 mmol). ^{1}H NMR ($CDCl_3$, 300 MHz, δ ppm): 7.26–7.30 (m, 5H); 7.35(t, J=9 Hz, 1H); 6.52 (s, 1H); 4.99 (d, J=9 Hz, 1H); 3.78–3.90 (m, 3H); 1.71 (s, 6H); 1.59–1.68 (m, 3H); 1.52 (s, 9H); 0.94–0.99 (m, 6H). Elemental Analysis Calcd for $C_{24}H_{37}N_3O_6$ (463): C, 62.20; H, 7.99; N, 9.07. Found: C, 62.28; H, 7.95; N, 10.17.

4.1.15. Boc-Leu(1)-Aib(2)-Gly(3)-OH 17. To Boc-Leu(1)-Aib(2)-Gly(3)-OBz **16** (4.63 g, 10 mmol), methanol (50 mL) and of 2 M NaOH (20 mL) were added and the progress of saponification was monitored by thin layer chromatography (TLC). The reaction mixture was stirred at room temperature. After 10 h methanol was removed under vacuum, the residue was taken in 50 mL of water, washed with diethyl ether (2×50 mL). Then pH of the aqueous layer was adjusted to 2 by adding 1 M HCl and it was extracted with ethyl acetate (3×40 mL). The extracts were pooled, dried over anhydrous sodium sulfate and evaporated under vacuum to yield a white solid.

Yield=70% (2.60 g, 7 mmol). Mp 140–142 °C. ^{1}H NMR ($(CD_3)_2SO$, 300 MHz, δ ppm): 12.38 (br, 1H); 8.02 (s, 1H); 7.72 (t, J=5 Hz, 1H); 7.01 (d, J=6 Hz, 1H); 3.83–3.91 (m,

2H); 3.53–3.61 (m, 1H); 1.52–1.60 (m, 3H); 1.44 (s, 6H); 1.37 (s, 9H); 0.84–0.89 (m, 6H). Elemental Analysis Calcd for $C_{17}H_{31}N_3O_6$ (373): C, 54.69; H, 8.31; N, 11.26. Found: C, 54.67; H, 8.16; N, 11.12.

4.1.16. Boc-Leu(1)-Aib(2)-Gly(3)-Aib(4)-OMe 4. To **17** (1.30 g, 5 mmol) in DMF (10 mL) was cooled in an ice water bath. H-Aib-OMe was isolated from the corresponding methyl ester hydrochloride (1.53 g, 10 mmol) by neutralization, subsequent extraction with ethyl acetate and concentration (7 mL) and this was added to the reaction mixture, followed immediately by DCC (1 g, 5 mmol) and HOBt (0.7 g, 5 mmol). The reaction mixture was stirred for 3 days. The residue was taken in ethyl acetate (50 mL) and DCU was filtered off. The organic layer was washed with 2 M HCl (3×50 mL), brine, 1 M sodium carbonate (3×50 mL), brine (2×50 mL), dried over anhydrous sodium sulfate and evaporated in vacuum to yield 2.25 g (4 mmol, 80%) of white solid. Purification was done by silica gel column (100–200 mesh) using ethyl acetate as eluent. Single crystals were obtained from methanol–water (methanol/water=90:10) by slow evaporation.

Yield=80% (1.90 g, 4 mmol). R_f (ethyl acetate) 0.68. Mp 145–147 °C. ν_{max} (KBr)/cm^{-1} 1657, 1728, 3273, 3368. ^{1}H NMR (10% $(CD_3)_2SO$ in $CDCl_3$, 300 MHz, δ ppm): 8.05 (s, 1H); 7.73 (t, J=11 Hz, 1H); 7.56 (s, 1H); 6.23 (d, J=6 Hz, 1H); 3.99–4.04 (m, 2H); 3.83–3.9 (m, 1H); 3.65 (s, 3H); 1.50–1.55 (m, 3H); 1.48 (6H, s); 1.47 (s, 6H); 1.44 (s, 9H); 0.92–0.97 (m, 6H). ^{13}C NMR ($CDCl_3$, 300 MHz, δ ppm): 174.98, 174.18, 173.25, 169.00, 156.61, 80.89, 56.95, 55.83, 54.47, 52.19, 43.32, 28.19, 25.63, 25.11, 24.96, 24.92, 24.66, 22.78, 21.89. $[\alpha]_D^{25.7}=-19.93$ (c 2.06, $CHCl_3$). Mass Spectral data $(M+Na)^+=495.5$. Elemental Analysis Calcd for $C_{22}H_{40}N_4O_7$ (472): C, 55.93; H, 8.74; N, 11.86. Found: C, 54.88; H, 8.77; N, 11.89.

4.1.17. Boc-γ-Abu(1)-OH 18. See Ref. 17.

4.1.18. Boc-γ-Abu(1)-Aib(2)-OMe 19. See Ref. 17.

4.1.19. Boc-γ-Abu(1)-Aib(2)-OH 20. See Ref. 17.

4.1.20. Boc-γ-Abu(1)-Aib(2)-Leu(3)-OMe 21. Boc-γ-Abu(1)-Aib(2)-OH (1.0 g, 3.5 mmol) in DMF (5 mL) was cooled in an ice-water bath and H-Leu-OMe was isolated from the corresponding methyl ester hydrochloride (1.27 g, 7 mmol) by neutralization, subsequent extraction with ethyl acetate and concentration (10 mL) and it was added to the reaction mixture, followed immediately by DCC (0.721 g, 3.5 mmol) and HOBt (0.472 g, 3.5 mmol). The reaction mixture was stirred for 3 days. The residue was taken in ethyl acetate (60 mL) and the DCU was filtered off.The organic layer was washed with 2 M HCl (3×50 mL), brine, 1 M sodium carbonate (3×50 mL), brine (2×50 mL), dried over anhydrous sodium sulfate and evaporated under vacuum to yield 1.23 g (2.9 mmol) of white solid.

Yield=85% (1.23 g, 2.9 mmol). Mp 134–136 °C. ^{1}H NMR ($CDCl_3$, 300 MHz, δ ppm): 7.35 (d, J=9 Hz, 1H); 6.49 (s, 1H); 4.76 (t, J=9 Hz, 1H); 4.63–4.56 (m, 1H); 3.71 (s, 3H); 3.20–3.18 (m, 2H); 2.21–2.19 (m, 2H); 1.79–1.82 (m, 2H); 1.61–1.64 (m, 3H); 1.53 (s, 3H); 1.55 (s, 3H); 1.45 (s, 9H); 0.99–0.92 (m, 6H). Elemental Analysis Calcd for $C_{20}H_{37}N_3O_6$ (415): C, 57.83; H, 8.91; N, 10.12. Found: C, 57.50; H, 8.40; N, 10.00.

4.1.21. Boc-γ-Abu(1)-Aib(2)-Leu(3)-OH 22. To Boc-γ-Abu(1)-Aib(2)-Leu(3)-OMe **21** (1.23 g, 2.9 mmol), MeOH (5 mL) and 2 M NaOH (3 mL) were added and the progress of saponification was monitored by thin layer chromatography (TLC). The reaction mixture was stirred at room temperature. After 10 h methanol was removed under vacuum, the residue was taken in 50 mL of water, washed with diethyl ether (2×50 mL). Then the pH of the aqueous layer was adjusted to 2 using 1 M HCl and it was extracted with ethyl acetate (3×50 mL). The extracts were pooled, dried over anhydrous sodium sulfate, and evaporated under vacuum to yield 0.9 g of Boc-γ-Abu(1)-Aib(2)-Leu(3)-OH as white solid.

Yield=77.58% (0.9 g, 2.25 mmol). Mp 203–205 °C. ^{1}H NMR ($(CD_3)_2SO$, 300 MHz, δ ppm): 12.34 (br, 1H); 7.75 (s, 1H); 7.58 (d, J=6 Hz, 1H); 6.81 (t, J=5.4 Hz, 1H); 4.23–4.15 (m, 1H); 2.95–2.89 (m, 2H); 2.01–2.15 (m, 2H); 1.61–1.54 (m, 2H); 1.54–1.50 (m, 3H); 1.31 (s, 9H); 1.37 (s, 6H); 0.87–0.79 (m, 6H). Elemental Analysis Calcd for $C_{19}H_{35}N_3O_6$ (401): C, 54.85; H, 8.72; N, 10.47. Found: C, 54.30; H, 8.40; N, 10.20.

4.1.22. Boc-γ-Abu(1)-Aib(2)-Leu(3)-Aib(4)-OMe 5. Boc-γ-Abu(1)-Aib(2)-Leu(3)-OH (0.8 g, 2 mmol) in DMF (5 mL) was cooled in an ice-water bath and Aib-OMe was isolated from the corresponding methyl ester hydrochloride (0.614 g, 4 mmol) by neutralization, subsequent extraction with ethyl acetate and concentration (10 mL) and it was added to the reaction mixture, followed immediately by DCC (0.412 g, 2 mmol) and HOBt (0.270 g, 2 mmol). The reaction mixture was stirred for 3 days. The residue was taken in ethyl acetate (60 mL) and the DCU was filtered off. The organic layer was washed with 2 M HCl (3×50 mL), brine, 1 M sodium carbonate (3×50 mL), brine (2×50 mL), dried over anhydrous sodium sulfate and evaporated under vacuum to yield 0.75 g (1.5 mmol) of white solid. Purification was done by silica gel column (100–200 mesh) using ethyl acetate as eluent. Single crystals were obtained from methanol–water (methanol/water=90:10) by slow evaporation.

Yield=75% (0.75 g, 1.5 mmol). R_f (ethyl acetate) 0.72. Mp 104–106 °C. ν_{max} (KBr)/cm^{-1} 1651, 1692, 1746, 3296. ^{1}H NMR ($(CD_3)_2SO$, 300 MHz, δ ppm): 7.54 (d, J=9 Hz, 1H); 7.41 (s, 1H); 6.08 (s, 1H); 4.70 (t, J=9.5 Hz, 1H); 4.5.–4.42 (m, 1H); 3.70 (s, 3H); 3.28–3.23 (m, 2H); 2.32–3.28 (m, 2H); 2.17–2.14 (m, 1H); 1.94–1.88 (m, 1H); 1.57 (s, 3H); 1.54 (s, 3H); 1.48 (s, 6H); 1.46 (s, 9H); 0.91–0.86 (m, 6H). ^{13}C NMR ($CDCl_3$, 300 MHz, δ ppm): 175.16, 174.27, 173.00, 172.00, 157.04, 141.39, 104.48, 79.62, 56.90, 55.92, 52.20, 51.70, 38.94, 38.39, 32.37, 28.36, 27.00, 26.42, 25.35, 24.94, 24.49, 23.72, 23.29, 20.84. $[\alpha]_D^{25.7}=-21.61$ (C 2.04, $CHCl_3$). Mass Spectral data $(M+H)^+=501.4$, $M_{calcd}=500$. Elemental Analysis Calcd for $C_{22}H_{44}N_4O_7$ (500): C, 57.60; H, 8.80; N, 11.20. Found: C, 57.12; H, 8.40; N, 10.94.

4.2. Single crystal X-ray diffraction study

For peptides **1**–**5**, intensity data were collected with MoKα radiation using the MARresearch Image Plate System. For all peptides, the crystals were positioned at 70 mm from the Image Plate. Selected details of the structure solutions and refinements are given in Table 3. 100 frames were measured at 2° intervals with a counting time of 2 min. Data analyses were carried out with the XDS program.[19] The structures were solved using direct methods with the Shelx86[20] program. For peptide **4**, the *t*-butyl group was disordered, each methyl group taking up two different sites each refined with 50% occupancy. For peptide **5** some atoms had high thermal parameters but no satisfactory disordered model could be obtained. Apart from disordered atoms, all non-H atoms were refined with anisotropic thermal parameters. The hydrogen atoms bonded to nitrogen and carbon were included in geometric positions and given thermal parameters equivalent to 1.2 times those of the atom to which they were attached. Those bonded to the water molecules in **5** could not be located. The structures were refined on F^2 using Shelxl.[21] Crystallographic data have been deposited at the Cambridge Crystallographic Data Centre reference CCDC 254598-254602 for peptides **1**–**5**.

Acknowledgements

We thank EPSRC and the University of Reading, U.K. for funds for the Image Plate System. S. Ray thanks the Council for Scientific and Industrial Research (C.S.I.R), New Delhi, India for financial assistance. This research is also supported by a grant from Department of Science and Technology (DST), India [Project No. SR/S5/OC-29/2003].

References and notes

1. Watson, J. D.; Crick, F. C. H. *Nature* **1953**, *171*, 737–738.
2. Ramachandran, G. N.; Kartha, G. *Nature* **1955**, *179*, 593–595.
3. Franklin, R. E. *Nature* **1955**, *175*, 379–381.
4. (a) Goldsbury, C.; Goldie, K.; Pellaud, J.; Seelig, J.; Frey, P.; Müller, S. A.; Kister, J.; Cooper, G. J. S.; Aebi, U. *J. Struct. Biol.* **2000**, *130*, 352–362. (b) Arvinte, T.; Cudd, A.; Drake, A. F. *J. Biol. Chem.* **1993**, *268*, 6415–6422. (c) Blanch, E. W.; Morozova-Roche, L. A.; Cochran, D. A. E.; Doing, A. J.; Hect, L.; Barron, L. D. *J. Mol. Biol.* **2000**, *301*, 553–563. (d) Sadqi, M.; Herna'ndez, F.; Pan, U. M.; Pe'rez, M.; Schaeberle, M. D.; Avila, J.; Munoz, V. *Biochemistry* **2002**, *41*, 7150–7155.
5. (a) Berl, V.; Huc, I.; Khoury, R. G.; Krische, M. J.; Lehn, J. M. *Nature* **2000**, *407*, 720–723. (b) Kolomiets, E.; Berl, V.; Odrizola, I.; Stadler, A.-M.; Kyritskas; Lehn, J. M. *Chem. Commun.* **2003**, 2868–2869.
6. (a) Hanessian, S.; Gomtsyan, A.; Simard, M.; Roelens, S. *J. Am. Chem. Soc.* **1994**, *116*, 4495–4496. (b) Hanessian, S.; Simard, M.; Roelens, S. *J. Am. Chem. Soc.* **1995**, *117*, 7630–7645.
7. (a) Rowan, I. E.; Notle, R. J. M. *Angew. Chem., Int. Ed.* **1998**, *37*, 62–68. (b) Feiters, M. C.; Notle, R. J. M. *Adv. Supramol. Chem.* **2000**, *6*, 41–156. (c) Lehn, J. M. *Chem. Eur. J.* **2000**, *6*, 2097–2102. (d) Lightfoot, M. P.; Mair, F. S.; Pritchard, R. G.; Warren, J. E. *Chem. Commun.* **1999**, 1945–1946. (e) Tobellion, F. M.; Seidel, S. R.; Arif, A. M.; Stang, P. J. *J. Am. Chem. Soc.* **2001**, *123*, 7740–7741.
8. Lehn, J. M.; Rigault, A.; Siegel, J.; Harrowfield, J.; Chevrier, B.; Moras, D. *Proc. Natl. Acad. Sci. U.S.A.* **1987**, *84*, 2565–2569.
9. (a) Allen, W. E.; Fowler, C. J.; Lynch, V. M.; Sessler, J. L. *Chem. Eur. J.* **2001**, *7*, 721–729. (b) Geib, S. J.; Vicent, C.; Fan, E.; Hamilton, A. D. *Angew. Chem., Int. Ed. Engl.* **1993**, *32*, 119–121.
10. Wang, Z.; Enkelmann, V.; Negri, F.; Mullen, K. *Angew. Chem., Int. Ed.* **2004**, *43*, 1972–1975.
11. (a) Moriuchi, T.; Nomoto, A.; Yoshida, K.; Ogawa, A.; Hirao, T. *J. Am. Chem. Soc.* **2001**, *123*, 68–75. (b) Nomoto, A.; Moriuchi, T.; Yamazaki, S.; Ogawa, A.; Hirao, T. *Chem. Commun.* **1998**, 1963–1964.
12. (a) Moriuchi, T.; Nishiyama, M.; Yoshida, K.; Ishikawa, T.; Hirao, T. *Org. Lett.* **2001**, *3*, 1459–1461. (b) Moriuchi, T.; Nomoto, A.; Yoshida, K.; Ogawa, A.; Hirao, T. *J. Am. Chem. Soc.* **2001**, *123*, 68–75.
13. (a) Parthasarathy, R.; Chaturvedi, S.; Go, K. *Proc. Natl. Acad. Sci. U.S.A.* **1990**, *87*, 871–875. (b) Ramasubbu, N.; Parthasarathy, R. *Biopolymers* **1989**, *28*, 1259–1269.
14. (a) Haldar, D.; Maji, S. K.; Sheldrick, W. S.; Banerjee, A. *Tetrahedron Lett.* **2002**, *43*, 2653–2656. (b) Haldar, D.; Maji, S. K.; Drew, M. G. B.; Banerjee, A.; Banerjee, A. *Tetrahedron Lett.* **2002**, *43*, 5465–5468. (c) Maji, S. K.; Banerjee, A.; Drew, M. G. B.; Haldar, D.; Banerjee, A. *Tetrahedron Lett.* **2002**, *43*, 6759–6762. (d) Banerjee, A.; Maji, S. K.; Drew, M. G. B.; Haldar, D.; Banerjee, A. *Tetrahedron Lett.* **2003**, *44*, 699–703. (e) Haldar, D.; Banerjee, A.; Drew, M. G. B.; Das, A. K.; Banerjee, A. *Chem. Commun.* **2003**, 1406–1407.
15. (a) Banerjee, A.; Maji, S. K.; Drew, M. G. B.; Haldar, D.; Banerjee, A. *Tetrahedron Lett.* **2003**, *44*, 335–339. (b) Maji, S. K.; Haldar, D.; Drew, M. G. B.; Banerjee, A.; Das, A. K.; Banerjee, A. *Tetrahedron* **2004**, *60*, 3251–3259.
16. (a) Karle, I. L.; Balaram, P. *Biochemistry* **1990**, *29*, 6747–6756. (b) Sacca, B.; Formaggio, F.; Crisma, M.; Toniolo, C.; Gennaso, R. *Gazz. Chim. Ital.* **1997**, *127*, 495–500. (c) Toniolo, C.; Crisma, M.; Formaggio, F.; Peggion, C. *Biopolymers (Pept. Sci.)* **2001**, *60*, 396–419.
17. Maji, S. K.; Banerjee, R.; Velmurugan, D.; Razak, A.; Fun, H. K.; Banerjee, A. *J. Org. Chem.* **2002**, *67*, 633–639.
18. Karle, I. L.; Banerjee, A.; Bhattacharjya, S.; Balaram, P. *Biopolymers* **1996**, *38*, 515–526.
19. Kabsch, W. *J. Appl. Crystallogr.* **1988**, *21*, 916.
20. Sheldrick, G. M. *Acta Crystallogr. Sect. A: Fundam. Crystallogr.* **1990**, *46*, 467.
21. Sheldrick, G. M. *Program for Crystal Structure Refinement*; University of Göttingen: Germany, 1993.